Experimental Validation of Interference Alignment Techniques using a Multiuser MIMO Testbed

Ó. González, D. Ramírez and I. Santamaria
Dept. of Communications Engineering
University of Cantabria
39005 Santander, Spain
Email: {oscargf, ramirezgd, nacho}@gtas.dicom.unican.es

J. A. García-Naya and L. Castedo
Dept. of Electronics and Systems
University of A Coruña
15071 A Coruña, Spain
Email: {jagarcia, luis}@udc.es

***Abstract*—Hardware platforms and testbeds are an essential tool to evaluate, in realistic scenarios, the performance of wireless communications systems. In this work we present a multiuser Multiple-Input Multiple-Output (MIMO) testbed made up of 6 nodes, each one with 4 antennas, which allows us to evaluate Interference Alignment (IA) techniques in indoor scenarios. We specifically study the performance of IA for the 3-user interference channel in the 5 GHz band. Our analysis identifies the main practical issues that potentially degrade the IA performance such as channel estimation errors or collinearity between the desired signal and interference subspaces.**

***Index Terms*—MIMO testbed, interference channel, interference alignment.**

I. Introduction

Interference alignment (IA) has recently emerged as an attractive transmission technique for the K-user interference channel [1]. Signals transmitted by all users are designed in such a way that the interfering signals at each receiver fall into a reduced-dimensional subspace. The receivers can then apply an interference-suppression filter to project the desired signal onto the interference-free subspace and, hence, the number of interference-free signalling dimensions of the network is substantially increased.

To better understand the impact of IA techniques on practical wireless networks, it is important to evaluate their performance in real-world scenarios rather than on simplistic channel models often used in simulation-based approaches (e.g. spatially uncorrelated channels, perfect synchronization among users, ...). However, experiments for the K-user Multiple-Input Multiple-Output (MIMO) interference channel require an extremely complex set-up made up of $2K$ MIMO terminals (K transmitters and K receivers). Complexity is considerably larger than in point-to-point MIMO links or in other multiuser MIMO scenarios such as the broadcast multiple-access channels. For instance, the simplest 3-user interference network requires six MIMO nodes with at least two antennas per node.

The cost associated to the required hardware set-up explains why the experimental evaluation of IA techniques reported in the literature is scarce, so far. To the best of our knowledge, the first experimental work on IA was presented in [2] where a technique that combines Interference Alignment and Cancellation (IAC) was implemented in a testbed made up of 20 GNU Radio Universal Software Radio Peripheral (USRP) nodes with two antennas each. Several practical issues have been evaluated in this work, such as the impact of different modulations, frequency/time synchronization aspects, or the idea of applying the alignment at the sample level (i.e., before timing and frequency offset correction). However, this technique requires an additional wired Ethernet connection to transfer already decoded packets between access points in order that some streams be cancelled.

Another experimental study on IA has been recently presented in [3]. Specifically, this work focuses on MIMO Orthogonal Frequency Division Multiplexing (MIMO-OFDM) 3-user interference channels measured in indoor and outdoor scenarios. The set-up comprises five National Instruments [4] PXI-1045 chassis connected to 3 PCs. Using the measured channels, IA techniques were evaluated in an off-line fashion. This work validates the feasibility of IA techniques and also evaluates the performance degradation under spatially correlated channels. However, notice that in [3] no aligned streams are actually transmitted over the wireless channel and, thus, many practical issues such as synchronization or hardware impairments are not taken into account.

In this paper we will present new IA experiments performed in the 5 GHz band. Specifically, we have focused on indoor 3-user interference wireless channels where each user sends one stream and is equipped with two antennas at both sides of the link. For this scenario, which is typically denoted as $(2\times 2, 1)^3$, closed-form IA solutions exist and can be obtained solving an eigenvalue problem. The conducted experiments use specifically designed frames and comprise two steps: i) a training step, where all pairwise interference channels are estimated and the corresponding IA precoders are obtained; and ii) a payload transmission step, where all users transmit concurrently using their IA precoders as well as a sequential Time Division Multiple Access (TDMA) mode that is used as a benchmark for comparison purposes.

This paper is organized as follows. Section II briefly presents the signal model and the IA technique, including the IA solution for the $(2 \times 2, 1)^3$ scenario. Section III describes the most important practical issues that can affect the IA real-world performance. The testbed hardware used for the experiments is described in Section IV, while the measurement set-up and methodology is described in Section V. The

978-1-61284-074-1/11/$26.00 ©2011 IEEE

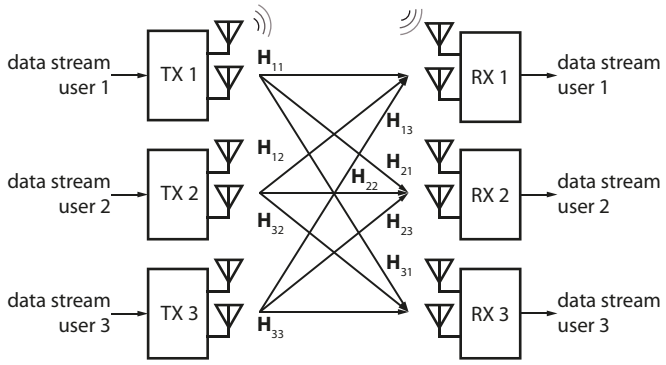

Fig. 1. Scheme of the $(2 \times 2, 1)^3$ interference network.

performance results are analyzed in Section VI considering the effects of the mentioned practical impairments. Finally, Section VII is devoted to the concluding remarks.

II. Interference Alignment for the 2×2 MIMO 3-user Channel

Let us consider a 3-user interference channel comprised of three transmitter–receiver pairs (links) that interfere with each other as shown in Figure 1. We assume that the three users wish to send one stream of data and are equipped with two antennas at each side of the link. The discrete-time signal at receiver i is the superposition of the signals transmitted by the three users, weighted by their respective channel gains and affected by noise, i.e.

$$\mathbf{y}_i = \mathbf{H}_{ii}\mathbf{x}_i + \sum_{j \neq i} \mathbf{H}_{ij}\mathbf{x}_j + \mathbf{n}_i \tag{1}$$

where $\mathbf{x}_i \in \mathbb{C}^{2\times 1}$ is the signal transmitted by the i-th user, $\mathbf{H}_{ij}$ is the 2×2 MIMO channel (assumed narrowband and time invariant) from transmitter j to receiver i, and $\mathbf{n}_i \in \mathbb{C}^{2\times 1}$ is the additive noise at receiver i.

Spatial domain IA is achieved if we are able to design a set of beamforming vectors (precoders) $\{\mathbf{v}_i \in \mathbb{C}^{2\times 1}\}$ and interference-suppression vectors (decoders) $\{\mathbf{u}_i \in \mathbb{C}^{2\times 1}\}$ such that, for $i = 1, \ldots, 3$,

$$\mathbf{u}_i^H \mathbf{H}_{ij}\mathbf{v}_j = 0, \quad \forall j \neq i \tag{2}$$

$$\mathbf{u}_i^H \mathbf{H}_{ii}\mathbf{v}_i \neq 0. \tag{3}$$

There exists a three-step analytical procedure to obtain the precoders and decoders for the $(2 \times 2, 1)^3$ case [1]:

1) The precoder for user 1, $\mathbf{v}_1$, is any eigenvector (each one yields a distinct IA solution) of the following 2×2 matrix,

$$(\mathbf{H}_{31})^{-1}\mathbf{H}_{32}(\mathbf{H}_{12})^{-1}\mathbf{H}_{13}(\mathbf{H}_{23})^{-1}\mathbf{H}_{21}. \tag{4}$$

2) The precoders for users 2 and 3, $\mathbf{v}_2$ and $\mathbf{v}_3$, are obtained respectively as

$$\mathbf{v}_2 = (\mathbf{H}_{32})^{-1}\mathbf{H}_{31}\mathbf{v}_1, \tag{5}$$

and

$$\mathbf{v}_3 = (\mathbf{H}_{23})^{-1}\mathbf{H}_{21}\mathbf{v}_1. \tag{6}$$

3) Finally, the interference-suppression filters (decoders) are designed to lie in the orthogonal subspace of the received signal, hence passing up the desired signal and cancelling the interference.

When precoders and decoders are applied at both sides of the link, the i-th user received signal is

$$\begin{aligned}\mathbf{r}_i &= \mathbf{u}_i^H \mathbf{H}_{ii}\mathbf{v}_i s_i + \sum_{j\neq i} \mathbf{u}_i^H \mathbf{H}_{ij}\mathbf{v}_j s_j + \mathbf{u}_i^H \mathbf{n}_i \\ &= \mathbf{u}_i^H \mathbf{H}_{ii}\mathbf{v}_i s_i + \mathbf{u}_i^H \mathbf{n}_i,\end{aligned}$$

where s_i is the 1-dimensional signal vector of the i-th TX node. Notice that the signal from the i-th transmitter to the i-th receiver travels through an equivalent Single-Input Single-Output (SISO) channel, $\mathbf{u}_i^H \mathbf{H}_{ii}\mathbf{v}_i$, and the interference terms have been perfectly suppressed by projecting the received signal onto the subspace whose basis is $\mathbf{u}_i$.

III. Practical Issues on Interference Alignment

Although IA has recently emerged as a fruitful field of theoretical work, few references exist in the literature that address their practical implementation. The reason for this is that the measurement equipment is expensive and lacks flexibility.

The first work on studying the performance of IA in a real setting is [2], where a hybrid version of IA coupled with interference cancellation and successive decoding is successfully tested. The work in [3] has also provided additional insight on the IA real-world feasibility by evaluating its sum-rate performance over measured MIMO channels. This work shows, via simulation over the measured channels, that IA is able to achieve the maximum multiplexing gain in the 3-user interference channel and, hence, it is optimal in the high SNR regime for different degrees of channel spatial correlation.

However, other practical impairments affect IA performance:

- In general, IA has a heavy reliance on network-wide channel state information. This can be directly observed from Eqs. (4) to (6), where the precoders and decoders design depends on all the interfering channels. In practice, this causes two different problems. The most obvious one is that the IA solution is highly sensitive to channel estimation errors. An estimation error in any of the interfering channels modifies all precoders and decoders. The second problem is that global channel state information needs to be shared between all nodes in order to compute an alignment solution. This fact introduces a delay between the channel estimation stage and the actual IA transmission stage. During this time the channel may vary, outdating the estimates, especially when there are moving scatterers in the surroundings.
  Both aforementioned problems translate into channel estimates $\hat{\mathbf{H}}_{ij}$ that differ from the actual channel values, $\hat{\mathbf{H}}_{ij} \neq \mathbf{H}_{ij}$, and, as a result, the i-th user received signal is

$$\mathbf{r}_i = \hat{\mathbf{u}}_i^H \mathbf{H}_{ii}\hat{\mathbf{v}}_i s_i + \sum_{j\neq i} \hat{\mathbf{u}}_i^H \mathbf{H}_{ij}\hat{\mathbf{v}}_j s_j + \hat{\mathbf{u}}_i^H \mathbf{n}_i. \tag{7}$$

where the precoders and the decoders have been computed from the interference channels, i.e. $\{\hat{\mathbf{v}}_i\}$ and $\{\hat{\mathbf{u}}_i\}$. Notice that a non-zero interference term remains even after the projection onto the orthogonal subspace of the assumed interference.

- In the absence of channel estimation errors or channel time-variations, the received signal, $\mathbf{y}_i$, is projected onto the orthogonal subspace of the interference, hence, suppressing all interference. However, some part of the energy of the signal is likely to lie in the interference subspace and is also removed. In some cases, when there is a high collinearity between the desired signal and interference subspaces, the desired signal is significantly affected.
  This problem shows that, although perfect IA solutions only depend on the interfering channels, the direct channels $\mathbf{H}_{ii}$ must also be taken into account to avoid signal and interference collinearity.
- Practical channels may exhibit antenna correlations and gain differences among different links which can be favorable or detrimental for the alignment. Specifically, spatial correlation and path losses are detrimental for the transmission, especially when they degrade the direct links. However, in the interfering links, they help to reduce the aggregate interference and achieve a larger multiplexing gain.
- Theoretical works often assume that precoders and decoders are applied at symbol level (i.e. on a symbol-by-symbol basis). However, synchronization tasks on a practical receiver are performed at sample-level and, hence, are affected by interference. As a consequence, in order to get a successful synchronization, IA precoding and decoding must be applied at sample-level, that is, as the last and first task of the TX and RX signal processing chains, respectively (see Fig. 5).

Summarizing, practical issues such as channel estimation errors, channel correlations, path losses and other impairments translate into interference leakages affecting the overall IA performance. For that reason, practical experiments are necessary to assess the impact of these practical impairments on real-world IA networks.

IV. Testbed Description

Among the different available possibilities to assess the impact of IA techniques on practical wireless networks, we chose the testbed approach because we already have past experience on point-to-point MIMO testbeds [5] and because such an approach is based on solely transmitting and acquiring the signals in real-time. The remaining signal processing tasks are implemented off-line, hence, reducing the development time as well as the manpower required.

The cost associated to the hardware that is necessary to build a multiuser multi-node MIMO testbed is considerably high. For instance, building the simplest $(2\times2,1)^3$ interference network with three users requires six nodes with at least two antennas per node. For this reason, we decided to build a multiuser testbed by integrating two existing multiuser MIMO testbeds respectively developed at the Universities of A Coruña (UDC) and Cantabria (UC). The three transmitters (see top of Fig. 2) were built at the UDC while the three receivers (see bottom of Fig. 2) come from the testbed developed at the UC.

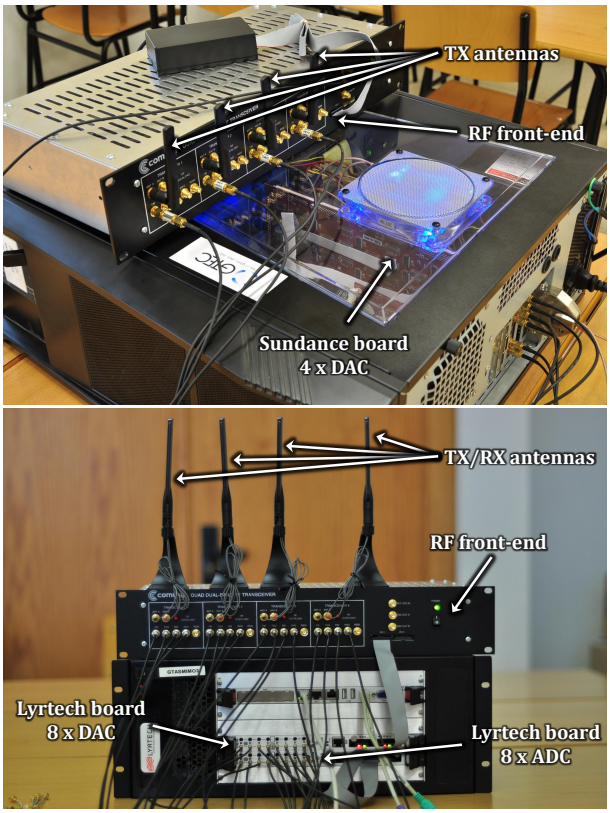

Fig. 2. Picture of a TX node (top) and a RX node (bottom).

Both transmit and receive testbed nodes are equipped with a Quad Dual-Band front-end from Lyrtech, Inc [6]. This Radio Frequency (RF) front-end can be equipped with up to eight antennas that are connected to four direct conversion transceivers by means of an antenna switch. The front-end is based on Maxim [7] MAX2829 chip (also found in front-ends like Ettus [8] XCVR2450 or Sundance [9] SMT911). It supports both up and down conversion operations from either a 2.4 to 2.5 GHz band or a 4.9 to 5.875 GHz band. The front-end also incorporates a programmable variable attenuator to control the transmit power value. The attenuation ranges from 0 to 31 dB in 1 dB steps, while the maximum transmit power declared by Lyrtech is 25 dBm per transceiver.

The baseband hardware of the three receivers is also from Lyrtech. More specifically, each node is equipped with a VHS-DAC module and a VHS-ADC module respectively containing eight Digital-to-Analog Converters (DACs) and eight Analog-to-Digital Converters (ADCs). Consequently, the receiver nodes can also be used as transmitters. Each pair of DAC/ADC is connected to a single transceiver of the RF front-end, and the signals are passed in I/Q format.

The baseband hardware of the the three transmitters is based

on Commercial Off-The-Shelf (COTS) components from Sundance Multiprocessor [9]. More specifically, each transmit node is based on the SMT8036E kit, containing four DACs that generate Intermediate Frequency (IF) signals that fed the RF front-end only through the I branch. Given that an IF signal is provided to a direct conversion front-end, at the output of the front-end we get the desired signal plus an undesired replica which is suppressed at the receiver by shifting the RF carrier frequency and by adequate filtering in the digital domain.

Both transmit and receive nodes make use of real-time buffers that are used to store the signals to be sent to the DACs as well as the signals acquired by the ADCs. The utilization of such buffers allows for the transmission and acquisition of the signals in real-time, while the signal generation and processing is carried out off-line. Additionally, both baseband hardware and RF front-ends of the transmit nodes are synchronized in time and in frequency by means of two mechanisms:

- Transmit nodes implement a hardware trigger attached to the real-time buffers and to the DACs. When one of the nodes switches on the trigger (usually the node corresponding to user 1), all buffers and DACs receive the trigger signal and simultaneously start to transmit.
- The same common external 40 MHz reference oscillator is utilized by both the DACs and the RF front-ends of all transmit nodes, thus guaranteeing the frequency synchronization.

The core component of each node is a host Personal Computer (PC) which allocates the baseband hardware and configures and controls the baseband hardware, as well as the RF front-end. Furthermore, the host PC provides remote control functionalities that allow the node to be externally controlled via an Ethernet connection. This flexible design has been found very useful for the integration of both testbeds, because each node can be transparently controlled without taking into account their particular technical differences. Also, it allows a so-called control PC with standard TCP/IP connections to use Matlab to interact with the whole testbed, which considerably enhances the development of multiuser experiments. Moreover, this control PC can act as a feedback channel to share channel state information between different users and it carries out all signal processing operations.

V. Measurement Set-up

Figure 3 shows a map of one of the lecture rooms of the Faculty of Informatics at the University of A Coruña. Such a set-up is utilized to emulate the interference network scheme shown in Figure 1. The three transmit nodes are located at the center of the room, each one separated nine meters away from the respective receive node. During the measurements (always carried out during night), the access to the room was controlled to ensure that there were no moving objects in the surroundings. Additionally, we also checked that the frequency bands measured at 5 GHz were clean and thus no other device was interfering. All nodes were equipped with monopole antennas at both transmitter and receiver sides. The antenna spacing is set to approximately seven centimeters

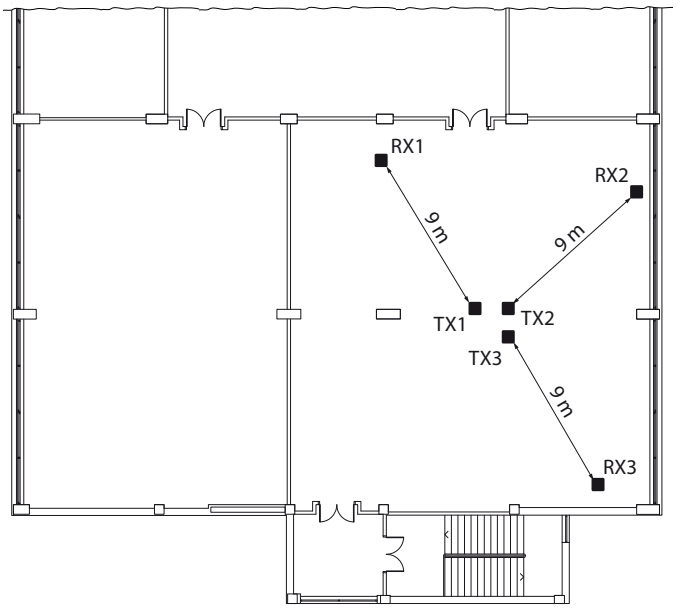

Fig. 3. Plan of the measured scenario: lecture room at the Faculty of Informatics, Campus de Elviña, A Coruña.

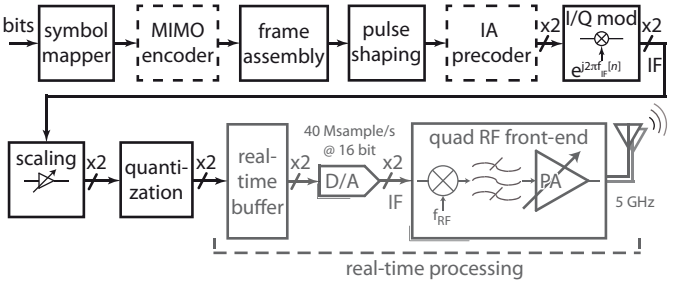

Fig. 4. Block diagram of hardware and software elements at each transmit node. The MIMO encoder and IA encoder are only applied during the training stage and the data transmission stage, respectively.

(forced by the separation of the antenna ports at the RF front-end).

The block diagram shown in Figure 4 shows the software and hardware elements utilized by each node at the transmit side to assess the aforementioned interference alignment scheme. The following steps are carried out:

- The source bits are mapped to a 4-QAM constellation (pilots employ a BPSK mapping).
- The resulting symbols are encoded, if required, in order to generate one symbol stream per transmit antenna.
- A Pseudo-Noise (PN) sequence is added as a preamble for synchronization in the frame assembly block.
- Up-sampling by a factor of 40, resulting in 40 samples per symbol.
- Pulse-shape filtering using a squared root-raised cosine filter with 40 % roll-off. Consequently, given that the sampling frequency of the DACs is set to 40 MHz, the resulting signal bandwidth is 1.4 MHz, which leads –according to our tests– to a frequency-flat channel response. Note

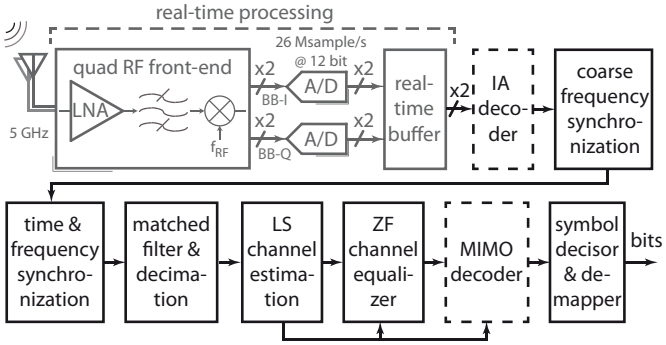

Fig. 5. Block diagram of hardware and software elements at each receive node. The MIMO decoder and IA decoder are only applied during the training stage and the data transmission stage, respectively.

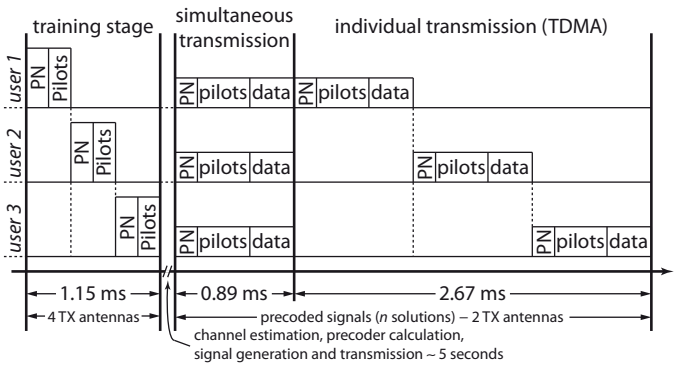

Fig. 6. Frame structure designed for the experimental evaluation of interference alignment schemes.

that the DACs implement an internal interpolating filter that improves the signal quality at the output, resulting in an actual sample rate of 160 Msample/s.
- If required, the transmit signals are precoded.
- The resulting signals are I/Q modulated to obtain a passband signal at a carrier frequency of 5 MHz.
- Such signals are then properly scaled in order to guarantee the transmit power level constraint.
- Given the 16 bits resolution of the DACs, the signals are properly quantized, obtaining 16-bit integer values for the samples.
- The resulting signals are stored off-line in the buffers available at the transmit nodes of the testbed (see Fig. 4).
- Once all signals are in the real-time buffers, the transmitter of the first user triggers all transmitters at the same time, and then all buffers are read simultaneously, cyclically, and in real-time by the corresponding DACs, hence generating signals at the IF of 5 MHz.
- The resulting analog signals are sent to the RF front-end to be transmitted at the desired RF center frequency. In our measurements we utilized 69 different carriers in the frequencies ranging from 5 200 MHz to 5 250 MHz and from 5 480 MHz to 5 700 MHz spaced 4 MHz each.

At the receiver side, once the transmitter has been triggered, the following steps are carried out at each receive node (see Fig. 5):

- The RF front-end down-converts the signals received by the selected antennas (up to four) to the baseband, generating the corresponding I and Q analog signals.
- All I and Q signals are then digitized by the ADCs by sampling at 26 MHz and, in real-time, they are stored in the corresponding buffers. Given that the signals are being transmitted cyclically and in order to guarantee that a whole frame is received, twice the length of the transmit frame is acquired.
- The signals are properly scaled according to the 12 bits ADC resolution. Notice that this factor is constant during the whole measurement, thus not affecting the properties of the channel.
- If required, the acquired signals are processed by the IA decoder.
- Next, coarse frequency synchronization followed by fine frequency synchronization and time synchronization are carried out.
- Once the acquired frames are correctly synchronized, the resulting signals are filtered and, as a result, discrete-time, complex-valued observations with 26 samples per symbol are obtained.
- After filtering, the signals are decimated. Instantaneous receive power as well as instantaneous power spectral density of the noise are estimated. During the evaluation stage, using all instantaneous values estimated, the mean Signal to Noise Ratio (SNR) is estimated.
- Finally, the frame is properly disassembled, and the resulting observations are then sent to the channel estimator and the channel equalizer.
- If required, the complex-valued signals are processed by the MIMO decoder.
- Finally, a symbol-by-symbol decisor followed by a demapper outputs the estimated bits.

A. Measurement Procedure

Figure 6 shows the structure of the frame designed to evaluate IA schemes with three transmit and three receive users. The measurement procedure consists of two steps: a training stage in which the channel is estimated, and a data transmission stage that consists of a simultaneous (IA) transmission and a sequential (TDMA) transmission. The TDMA phase is intended to evaluate the quality of interference-suppression in the same channel and synchronization conditions.

- During the training stage all nine pairwise MIMO channel matrices are estimated.
- Once all users acquire the signals transmitted during the training stage, channel estimation, precoder/decoder calculation and signal generation and distribution among the transmit nodes take place. Such operations take around five seconds to be completed. We will denote the MIMO channel estimates as $\hat{\mathbf{H}}_{ij}\ \forall i,j \in \{1,2,3\}$ and the calculated set of precoders and decoders as $\{\hat{\mathbf{v}}_i\}$ and $\{\hat{\mathbf{u}}_i\}$, respectively. The symbols $\hat{}$ over all variables

denote that they are estimates of the true MIMO channels, $\mathbf{H}_{ij}$, and the optimal precoders and decoders $\{\mathbf{v}_i\}$ and $\{\mathbf{u}_i\}$.

- During the data transmission stage, all transmit signals are IA precoded in both the IA and TDMA phases.
- At the receiver side, two different strategies are adopted:
  1) The IA decoders are applied in both IA and TDMA phases. The goal of this process is evaluating the performance degradation caused by the interference (IA phase) when compared with the performance achieved in absence of interference (TDMA phase). Furthermore, the sequential TDMA transmission allows to estimate the equivalent SISO channels at each link. These estimated SISO channels are denoted as $\hat{h}_{ij}$ and, in an ideal situation, should match the presumed channels obtained from the parameters estimated in the training stage, $\hat{\mathbf{u}}_i^H \hat{\mathbf{H}}_{ij} \hat{\mathbf{v}}_j$.
  2) In the TDMA phase, all the receivers are able to receive the signal from the rest of users. Then, each receiver is able to estimate three different Single-Input Multiple-Output (SIMO) channels, one per transmitter user. We will denote these SIMO channel estimates as $\hat{\mathbf{h}}_{ij}$. If no channel estimation errors or channel variations were present, these estimates should exactly match the presumed SIMO channels obtained in the training stage, $\hat{\mathbf{H}}_{ij}\hat{\mathbf{v}}_j$. The relative difference between both SIMO channel estimates allows us to calculate the channel estimation errors, E_{ij}:

$$E_{ij} = \frac{\|\hat{\mathbf{H}}_{ij}\hat{\mathbf{v}}_j - e^{j\hat{\theta}_{ij}}\hat{\mathbf{h}}_{ij}\|^2}{\|\hat{\mathbf{H}}_{ij}\hat{\mathbf{v}}_j\|^2} \tag{8}$$

  where the term $e^{j\hat{\theta}_{ij}}$ is used to correct the estimated phase difference that exists between both channel estimates, $\hat{\theta}_{ij}$. This phase difference is due to the lack of synchronization between the transmitter and receiver nodes and is not a problem for the alignment.

In order to simplify the evaluation stage, we always transmit at a high power level, but avoiding non-linear effects caused by the saturation of the power amplifiers and, at the same time, providing a mean received SNR value around 20 dB. This, on the one hand, ensures that the errors in the synchronization will not cause a significant impact on the observed results. On the other hand, the estimates of the channel will be accurate enough to extract meaningful conclusions.

B. Channel Realizations

The whole measurement campaign involves a large number of executions of the previously described procedure over different wireless channels. With the aim of obtaining statistically rich channel realizations, we make use of the following three techniques:

- Given that the Lyrtech RF front-end is frequency-agile, we measure at different RF carriers in the frequency interval ranging from 5 200 MHz to 5 250 MHz and from 5 480 MHz to 5 700 MHz. Carrier spacing is 4 MHz (greater than the signal bandwidth), which results in 69 different frequencies.
- For all 69 different frequencies, we measure using two different antenna sets attached to each front-end and controlled by means of the front-end antenna switch.
- Finally, given that the $(2 \times 2, 1)^3$ scheme requires only two transmit and two receive antennas per node, we can utilize either antennas 1 and 2 or antennas 3 and 4 of each front-end.

The combination of these techniques gives a total of $69 \times 2^6 \times 2^6 = 282\,624$ different channel realizations that can be obtained without moving the transmit nodes nor the receive nodes. Obviously, such a high number of measurements requires a lot of transmission and processing time. For that reason, we have restricted ourselves to around 1 000 measurements.

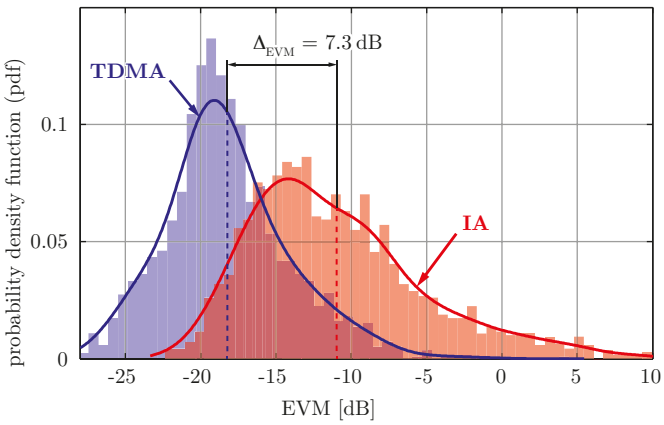

Fig. 7. Histogram and estimated pdf of the received signal constellations EVM for both IA and TDMA transmissions.

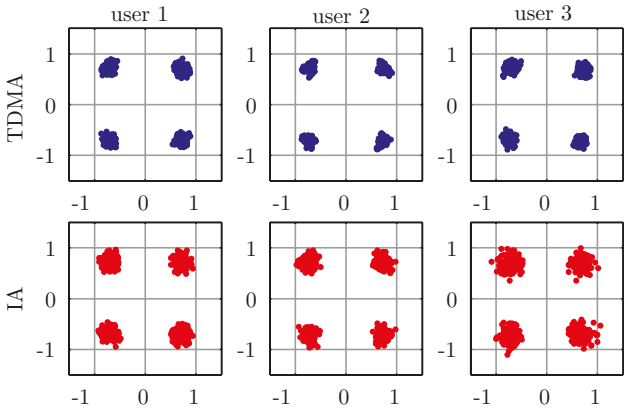

Fig. 8. Constellation comparison in absence of channel estimation errors and good SNR conditions.

VI. Results

In this section we summarize the results obtained from the mentioned measurement campaign.

A. Evaluation of the Constellation Quality through EVM Measurements

We have used the measurements collected to study how the aligned transmission affects the quality of the received signal. The metric that has been chosen to quantify that quality has been the Error Vector Magnitude (EVM) [10, Chapter 1, pp. 27] of the received signal constellations. Figure 7 shows the histogram and estimated probability density function (pdf) of the EVM measurements over the IA and TDMA constellations. It is shown that the mean EVM for TDMA is 7.3 dB better than that obtained from the IA transmissions. The obvious hypothesis that explains this result is that there exists a residual interference that causes the signal degradation. However, it is not clear what are the causes of this interference leakage.

Indeed, different degraded situations may occur. Figure 8 shows an example where IA performs similar to TDMA. From the TDMA phase, we have evaluated both the channel estimation errors, E_{ij}, (as defined in (7)) and the magnitude of the equivalent SISO channels, $|\hat{\mathbf{u}}_i^H \hat{\mathbf{h}}_{ij}|$. Specifically, the channel estimation errors for this channel are always lower than 2.4 %, which is lower than the average of the channel estimation errors in the full set of measurements. Furthermore, the magnitude of the worst direct link SISO channel is larger than 75 % of the full set of measurements. In summary, the good performance of IA in this example is due to the simultaneous fulfillment of two basic requirements: low channel estimation errors and good equivalent direct links.

Figure 9 shows an example where the magnitude of the equivalent channel for the user 2, $|\hat{\mathbf{u}}_2^H \hat{\mathbf{h}}_{22}|$, is very small. More specifically, the magnitude of the equivalent channel is lower than 25 % of the channel magnitudes in the full set of measurements. In other words, due to the high collinearity between desired signal and interference, a large amount of signal is lost when supressing the interference. As expected, the noise causes a degradation that can be also observed in the TDMA constellation.

In Figure 10 a new set of received constellations is shown. The one corresponding to user 1 is clearly affected by residual interference. It is caused by large estimation errors in the channel from transmitters 1 and 3 to receiver 2. More specifically there is a 20 % error in both estimates that is larger than the 90 % of the errors found in the full dataset. This large estimation error causes large interference leakages, specially from transmitter 2 to receiver 1 where the interference level is only 12 dB lower than the desired signal strength.

B. Evaluation of Sum-rate Performance

In this section we evaluate the sum-rate performance of TDMA and IA. Specifically, the achievable sum-rate for TDMA has been calculated as

$$\mathrm{SR}_{\mathrm{TDMA}} = \frac{1}{3}\sum_{i=1}^{3} \log_2\left(1 + \frac{|\hat{h}_{ii}|^2}{\sigma^2}\right) \tag{9}$$

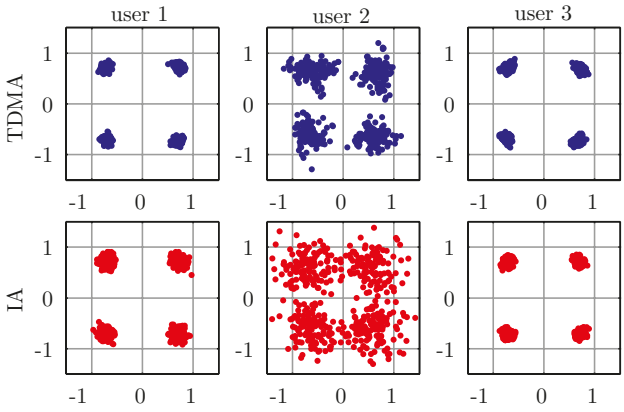

Fig. 9. Constellation comparison in a case where signal is highly collinear with the interference subspace.

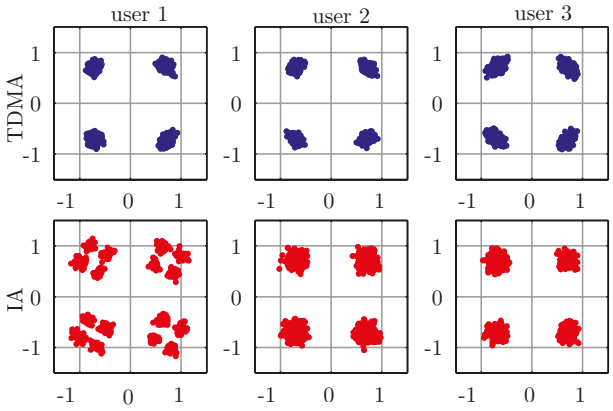

Fig. 10. Constellation comparison in presence of channel estimation errors.

where the following considerations are done:

- Each TDMA user communicates during one third of the transmission time.
- The equivalent SISO channel for the i-th user is $\hat{h}_{ii}$.
- The noise variance σ^2 is estimated during silence periods between frame transmissions.

On the other hand, the IA sum-rate is calculated as

$$\mathrm{SR}_{\mathrm{IA}} = \sum_{i=1}^{3} \log_2\left(1 + \frac{|\hat{h}_{ii}|^2}{\sigma^2 + \sum_{\substack{j=1 \\ j\neq i}}^{3} \|\hat{\mathbf{u}}_i^H \hat{\mathbf{h}}_{ij}\|^2}\right) \tag{10}$$

where the same considerations as before apply but, with the following exceptions:

- Each IA user communicates during the whole transmission time.
- The equivalent SISO channel for the interfering links is estimated as $\hat{\mathbf{u}}_i^H \hat{\mathbf{h}}_{ij}$ because it is imposible to be estimated after the actual interference-suppression. That is the reason why it is estimated from the SIMO channel estimates, $\hat{\mathbf{h}}_{ij}$ and then multiplied by the interference-suppression filter, $\hat{\mathbf{u}}_i^H$.

Figure 11 shows the complementary cumulative distribution function (ccdf) of the achievable sum-rates of both schemes.

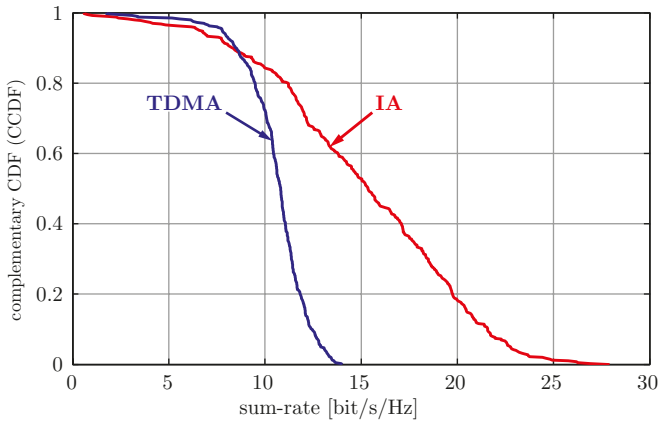

Fig. 11. ccdf of the sum-rate achievable by both the IA and TDMA strategies.

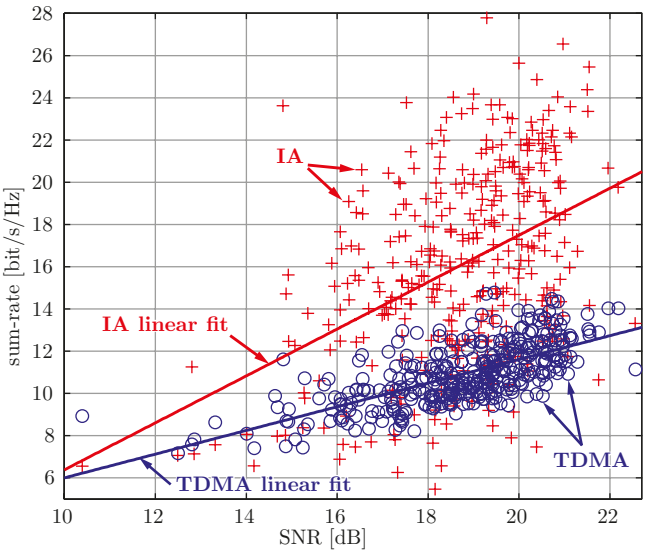

Fig. 12. Achievable sum-rate performance vs estimated SNR.

It can be seen that IA clearly outperforms TDMA. As an example, the sum-rate achieved by IA is larger than 15 bits/s/Hz for 50 % of the measurements, while TDMA never achieved this rate.

In Figure 12 the sum-rate estimations are plotted versus the measured SNR. Furthermore, a linear fit of both set of points is shown with the goal of computing the high SNR slope of the sum-rate curve. Theoretically, IA is expected to provide a high SNR slope that is three times the slope provided by TDMA. As a result of the performance degradations introduced by channel estimation errors and signal and interference collinearity, in the experimental results shown in Figure 12 the IA slope doubles that of TDMA.

VII. Conclusions

In this paper we have presented a multiuser MIMO testbed that has been built for verifying the real-world feasibility of the IA transmission methods. Also, a detailed description of the signal processing chains and measurement procedure is given. We have shown that the IA performance is degraded due to practical issues such as channel estimation errors and signal-interference collinearity. Furthermore, we have evaluated the sum-rate performance of IA showing that IA improves the multiplexing gain but the observed gains differ from those found through theory and simulation. Both results suggest that future theoretical work must be focused on designing robust or dynamic interference alignment algorithms to deal with channel estimation errors and direct link degradations.

Acknowledgments

This work has been funded by Xunta de Galicia, Ministerio de Ciencia e Innovación of Spain, and FEDER funds of the European Union under grants with numbers 10TIC003CT, 09TIC008105PR, TEC2010-19545-C04-01, TEC2010-19545-C04-02, AP2009-1105, AP2006-2965, and CSD2008-00010.

References

[1] V. Cadambe and S. Jafar, "Interference alignment and spatial degrees of freedom for the K user interference channel," in *Proc. IEEE International Conference on Communications (ICC 2008)*, pp. 971–975, May 2008, http://dx.doi.org/10.1109/ICC.2008.190doi: 10.1109/ICC.2008.190.

[2] S. Gollakota, S. D. Perli, and D. Katabi, "Interference alignment and cancellation," *SIGCOMM Comput. Commun. Rev.*, vol. 39, pp. 159–170, August 2009, http://dx.doi.org/10.1145/1594977.1592588doi: 10.1145/1594977.1592588.

[3] O. El Ayach, S. Peters, and R. W. Heath, "The feasibility of interference alignment over measured MIMO-OFDM channels," *Vehicular Technology, IEEE Transactions on*, vol. PP, no. 99, pp. 1 –1, 2010, http://dx.doi.org/10.1109/TVT.2010.2082005doi: 10.1109/TVT.2010.2082005.

[4] "National Instruments," 2011. http://www.ni.com

[5] D. Ramírez, I. Santamaría, J. Pérez, J. Vía, J. A. García-Naya, T. M. Fernández-Caramés, H. J. Pérez-Iglesias, M. González López, L. Castedo, and J. M. Torres-Royo, "A comparative study of STBC transmissions at 2.4 GHz over indoor channels using a 2x2 MIMO testbed," *Wireless Communications and Mobile Computing*, vol. 8, no. 9, pp. 1149–1164, Nov. 2008, http://dx.doi.org/10.1002/wcm.558doi: 10.1002/wcm.558.

[6] "Lyrtech, Inc." 2011. http://www.lyrtech.com

[7] "Maxim Integrated Products, Inc." 2011. http://www.maxim-ic.com/

[8] "Ettus Research, LLC," 2011. http://www.ettus.com

[9] "Sundance Multiprocessor, Ltd." 2011. http://www.sundance.com

[10] A. Behzad, Wireless LAN Radios. Hoboken, New Jersey, USA: John Wiley & Sons, 2007. http://at.bookbutler.com/do/bookCompare?searchFor=978-0471-70964-0amountIn=eurshipTo=atsearchIn=dezip=ISBN: 978-0471-70964-0.